

Porewater and solid phase speciation geochemistry of phosphorus in the Western Bay of Bengal: An assessment of depositional pathways

P. Linsy^{1,2}, B. Nagender Nath^{1*}, M.B.L. Mascarenhas-Pereira¹, Tyson Sebastian^{1,2}, B. Ramalingeswara Rao¹ Armoury Kazip¹, Durbar Ray¹, Saranya Jayachandran^{1,3}, L. Surya Prakash^{1,2}

¹CSIR-National Institute of Oceanography, Dona Paula, Goa 403 004, India

²National Centre for Polar and Ocean Research, Ministry of Earth Sciences, Goa, 403804, India

³Centre for Ocean, River, Atmosphere and Land Sciences, Indian Institute of Technology Kharagpur, West Bengal, India-721302

*Corresponding author email: nagendernath@yahoo.com

Abstract

In this study, we used a combination of porewater phosphate and solid-phase P speciation to examine the present-day benthic biogeochemical cycling and pathways of phosphorus (P) deposition at four sites in the western Bay of Bengal (BoB). We concentrate on two regions, with 2 sediment cores from each region. One is the Palar basin where ancient phosphorites and phosphatic grains were discovered before, and the other in the Cauvery basin, where no phosphorites are known to occur. Both of these regions fall in the depths of the oxygen minimum zone (OMZ). Our results suggest that the influx of lithogenic material, or lack of it, largely regulates the sedimentary cycling of P in BoB. Both locations lack active phosphogenesis due to substantial inputs of non-reactive P relative to reactive P from river runoff and its quick burial by the ballasting effect, which appears to prevent P from transforming into an authigenic phase. Despite the oxygen-depleted conditions, low bacterial respiration limits the microbial reduction of iron oxyhydroxide and makes the redox cycling of iron a weak player in the sedimentary cycling of P in the studied cores. The burial efficiency of P is relatively high in the Cauvery basin cores owing to the high sediment accumulation rate and suggests that most of the sedimentary P is undergoing burial with a minimum regeneration. Lack of/Very low recent sedimentation in the Palar basin is possibly due to the reported migration of river course towards the south during the mid-to Late Holocene.

Keywords: Porewater phosphate, Phosphorous Speciation, Sediment, Cauvery, Palar, Oxygen Minimum Zone, Productivity, Sedimentation

1. Introduction

Phosphorus (P) is a key element that limits marine primary productivity in short and long time scales (Holland, 1978; Howarth et al., 1995; Tyrrell, 1999). The major source of P to the oceans is fluvial input which brings weathered constituents. Only 30% of the fluvial P is biologically available for marine primary production because the majority of riverine P is trapped in estuaries and continental margins (Compton et al., 2000). However, it is feasible that remobilization of P that is buried in the marine sediments could boost primary production on its dissolution and release into the photic zone through benthic supply. Thus, it is important to study the P cycling in marine sediments. Studying P geochemistry of sediments in combination with porewater and overlying ocean water will help us in understanding the pathways of P cycling, remobilization and resultant bioavailability if any.

The Bay of Bengal (BoB) is a major recipient of dissolved elements and suspended material from major rivers draining the Himalaya and Peninsular India (Holeman, 1968; Milliman and Meade, 1983; Subramanian et al., 1985), and the riverine fluxes strongly influence the biogeochemistry in the area (Ittekkot et al., 1991; Rao et al., 1994). Similar to the Arabian Sea, BoB also possesses an oxygen minimum zone (OMZ) at intermediate depths (Rao et al., 1994; Sardesai et al., 2007) but at much shallower depths. The river inputs are the principal source of nutrients to the BoB, and the P supply from rivers in the region constitutes about 10% of the world's total inorganic P (Datta et al., 1999; Stoll et al., 2007).

Phosphorites, which are sedimentary deposits that contain more than 18 wt% of P_2O_5 (Compton and Bergh, 2016; Filippelli, 2011), were first reported to occur in the Bay of Bengal by Vaz (1995). They were recovered from the eastern continental margin of India off Chennai from a water depth of about 150m. Later, Vaz et al. (1999) and Rao et al. (1998, 2000, 2002) found phosphorite/phosphatic concretions at 30 to 300m water depths in an area covering about 636 km². The P_2O_5 content of these phosphorites ranged between 21.35 and 31.12 wt% (Rao et al., 1998). This is, by far, the largest phosphorite field reported on the continental margin of India (Vaz et al., 1999; Rao and Kessarkar, 2001). These phosphorites were associated with foraminiferal microfossils belonging to upper Cretaceous-lower Eocene age and pelecypod fossil casts of upper Cretaceous to Miocene age (Vaz, 1995) but have been attributed to microbial origin. Similarly, Rao et al. (2000, 2007) too have invoked the microbial processes, with microbial mats forming on the outer shelf and were phosphatized later. Based on subsequent work, Vaz et al. (1999) have proposed the occurrence of four episodes of phosphatization commencing from the Eocene period but has ruled out the phosphatization during the late Pleistocene and early Holocene period. Thus, unlike in the Arabian

Sea (Linsy et al., 2018b; Schenau et al., 2000), it is not known whether the present-day phosphogenesis or the recent phosphatization is occurring in the BoB.

A study by Sarma et al. (2020) suggests seawater phosphate severely limits nitrogen fixation in the BoB. They inferred that the removal of dissolved inorganic phosphate (DIP) within the estuaries before reaching the coast, low atmospheric input, and strong stratification are the potential reasons for phosphate limitation for N₂ fixation in the BoB. Rao et al. (2021) suggested that the potential removal of phosphate through the adsorption onto the suspended particulate matter removes ~5-50% of the total DIP and leads to a decrease in primary production in the BoB by ~1 to 2% (Sarma, 2022). While the removal of dissolved P through particle adsorption and sinking is established, the labile P in sediments can undergo dissolution under low oxygenated conditions, releasing dissolved phosphate to the seawater which can potentially be bioavailable. The sediments thus can act both as a source and sink of P (see Linsy et al., 2018a, 2018b). Studies on the geochemistry of P in the Bay of Bengal are limited. Babu and Ramaswamy (2017) studied the geochemistry of P in the surface sediments from the BoB and have reported the occurrence of higher P values in shelf sediments, compared to slope and deep-sea. Mohanty et al. (2018) studied the variability of P phases in offshore sediments from the Tamil Nadu coast, with both these studies focusing on the surface sediments and none dealt with porewater geochemistry and the subsurface changes in P sink pathways, leaving a significant gap in our understanding the role of early diagenesis on P cycling at sediment-water interface in the BoB. Thus, this study has been undertaken on sediment cores to assess the P regeneration and burial in the western BoB using porewater and solid phase speciation geochemistry of P. This is the first detailed study focusing on the benthic P dynamics in the BoB sediments with a view to examine the present day phosphogenesis, if any, and the depositional pathways of P within these sediment cores. For this, two sediment cores each from two areas in the western BoB, first one is a phosphorite bearing zone of the Palar basin and the second one in the Cauvery basin with no reported occurrences of phosphorites.

2. Materials and methods

2.1. Regional setting

The Eastern Continental Margin of India (ECMI) is a passive margin drained by numerous peninsular rivers which form three major sedimentary basins viz. Cauvery - Palar, Krishna-Godavari (KG), and Mahanadi (from south to north). The Cauvery Basin in the south-eastern Indian peninsula is situated between the latitudes 8°30' and 12°30'N and longitudes 78°30'E and 80°20'E (Narasimha Chari et al., 1995). The Palar Basin is situated between the Cauvery and the KG basins and stretches

from the Pulicat lake region in the north to Palar Canyon System in the south (Rangaraju et al., 1993; Susanth et al., 2021b; Twinkle et al., 2016). The Cauvery-Palar Basin exhibits drastic variations in the degree of slope. The Palar Basin is characterized by a very steep slope (gradient, 3°–78°) and high fault escarpment (Susanth et al., 2021b). In contrast, the continental slope of the Cauvery Basin is gentle, with narrow continental shelf. The Cauvery-Palar margin is marked by numerous submarine canyons, sinuous channels, sediment waves, mass transport complexes, etc. (Bastia et al., 2011; Susanth et al., 2021b).

2.1.1. Palar Basin

The Palar Basin drained by structurally controlled Palar river, is one of the major rivers in southern peninsular India. It occupies an area of 4000 km² on land and extends offshore towards the east where it covers an area of 2800 km² (Sastri et al., 1981). A great part of the lower Palar River basin encompasses thick beds of Quaternary sediments. The phosphorites were recovered over a large area (800 km²) on the outer shelf and slope regions of Palar Basin between 100 and 500 m water depth (Vaz et al., 1999; Vaz, 1995).

2.1.2. Cauvery Basin

The Cauvery Basin is drained by the Cauvery River, which originates in the Brahmagiri range of the Western Ghats and drains through the Precambrian formations of India comprised of the Dharwar system, Peninsular Indian granite gneiss, charnockite, and Closepet granite (Krishnan, 1982). Cauvery River travels 800 km through the basin, whose average annual rainfall is 1092 mm, before emptying its sediment load into the Bay of Bengal (Vaithiyanathan, 1990).

2.2. Sampling

Four short sediment cores were collected during the 50th (May 2013) and 59th (January 2014) cruises of RV Sindhu Sankalp from the eastern continental margin of India (**Fig. 1**). Two sediment cores were collected from the phosphorite-bearing area from the Palar basin and the remaining two from the non-phosphorite bearing area of the Cauvery basin, all overlain by oxygen-depleted waters. Seawater samples from these locations were also collected at pre-determined depths using a rosette sampler attached with 10L Niskin bottles. Water column temperature and salinity were measured with a conductivity temperature depth (CTD) profiler to which an oxygen sensor was attached (SBE 25, Seabird USA). The sediment samples were collected using a spade corer with dimensions of 30 cm x 15 cm x 50 cm.

Sediment cores for porewater extraction (two from each sampling site) were collected by pushing a plexiglass (6 cm diameter) into the collected sediment cores and were immediately

transferred into the N₂-purged glove chamber to ensure minimal contact with atmospheric oxygen. The sediment cores were sliced at a 2 cm interval and were centrifuged at 6000 rpm (4427 RCF) at in-situ temperatures (bottom water temperature) for 20 minutes in a refrigerated centrifuge. The supernatant porewater was filtered through 0.45 µm MILLEX HA syringe filters and stored at -20 °C. The sediment cores for geochemical analysis were stored at -20°C.

Dissolved phosphate concentration in porewater and seawater was measured onboard using the standard spectrophotometric method (Grasshoff et al., 1983). The procedure involves the reaction of phosphate with molybdate at a low pH; the phosphomolybdate that results is reduced by ascorbic acid to a blue complex that can be determined spectrophotometrically. Duplicate measurements were carried out for all samples, and the absorbance was measured at 880nm using a Shimadzu UV-1700 spectrophotometer with a 1-cm quartz cell. The calibration standards were prepared using the salt of Potassium dihydrogen phosphate (dried at 110 °C). The analytical error was monitored using a replicate analysis of the standard solution. Replicate analysis indicated that the relative error of dissolved phosphate measurement was generally less than 5%. Dissolved oxygen concentration in the seawater samples was measured by Winkler's titration method immediately after collection (Carritt and Carpenter, 1966). In order to minimize atmospheric contamination, DO samples were collected in ground-glass stopper bottles by filling them three times over with seawater. The DO samples were fixed using MnCl₂ and alkaline KI and analyzed onboard with a Metrohm Dosimat auto titrator. The dissolved oxygen data measured by Winkler's method, data compared well with CTD (make Sea Bird 911 Plus, USA) profiler DO sensor data and showed a strong positive correlation with R² value of >0.988.

2.3. Solid phase analysis

The sediment cores for geochemical analysis were sub-sampled at 1 cm intervals, freeze-dried, and ground with an agate mortar and pestle. Total inorganic carbon (TIC) in sediments was determined using a CO₂ coulometer (UIC coulometer-CM5015). Anhydrous Calcium carbonate (12 wt.% C) of 99% purity/assay (Merck make) was employed as a standard material for the TIC analysis. The precision and accuracy were assessed, and the error was better than 5%. Total carbon (TC) and total nitrogen (N_{total}) in sediments were measured with a CN analyzer (Thermo Scientific Flash 2000). The Soil Standard Clay OAS-B2184, certificate no:133317 (containing 0.021 wt. % .N and 2.29 wt.% C) of Elemental Microanalysis Limited was used as a standard for the calibration and accuracy determination and the error was within ±3%. Total organic carbon (C_{org}) was determined by subtracting TIC from TC..

Solid phase P fractionation was carried out using the sequential extraction procedure developed by Ruttenberg (1992) and modified by Babu and Nath (2005) by adding a step of Schenau and De Lange (2000) for biogenic P (including fish debris). The modified method (of Babu and Nath, 2005) was employed before to understand the present-day phosphogenesis in the Eastern Arabian Sea and the P species distribution in the Central Indian Basin (Linsy et al., 2018b, 2018a). 100 mg of each dry powdered sediment sample was repeatedly leached with 25 ml of 2 M NH_4Cl (pH 7; 8 times; 4 hrs) to extract exchangeable or loosely sorbed, carbonate-associated P and biogenic apatite (P_{bio}). In the second step, to separate easily reducible or reactive iron-bound P (P_{Fe}), the residue was washed with 10 ml citrate dithionite buffer (pH 7.6; 6 hrs), followed by 25 ml of 2 M NH_4Cl (pH 7; 2 hrs) and 10ml of distilled water (2hrs). For extracting authigenic apatite (P_{auth}), the residue was treated with 1 M sodium acetate buffer (pH 4; 6 hrs), 1 M MgCl_2 (pH 8; 2 hrs) and distilled water. P associated with a detrital fraction (P_{det}) was extracted by 1 M HCl (16 hrs). For extracting the P bound to organic matter (P_{org}), the residue was dried and heated with 50% (w/v) magnesium nitrate at 80°C and then combusted at 550°C (2 hrs). P_{org} was extracted by 1M HCl (24 hrs). After each extraction, the supernatant liquid was collected by centrifuging for 15 minutes at 5000 rpm, then transferred into plastic bottles that had been cleaned with acid.

The sequential extraction technique was carried out using analytical-grade reagents, and the extraction was done at room temperature. Milli Q system ultrapure water was used for the reagent preparation and final washing of the lab wares. To assess the reproducibility of the method, duplicates of the sample were used during the extraction. The relative standard deviations for analyses of P_{bio} and P_{Fe} ranged from 0.1 to 5.5%, while for P_{auth} it was between 0 and 8.5%, 1.8 and 6.3% for P_{det} , and for P_{org} it was between 0.37 and 4.1%. The recovery of the extraction was tracked using standard reference materials (Jlk-1 of the Geological Survey of Japan and MAG-1 of the United States of Geological Survey), and showed a recovery of 114% for Jlk-1 and 89% for MAG-1. P concentrations in all other phases were measured colorimetrically by the molybdenum blue method (Strickland and Parsons, 1972) except the P_{Fe} phase. For the measurement of P in P_{Fe} phases, an organic extraction method, reduction by stannous chloride developed by Watanabe and Olsen (1962), was adopted to prevent interferences from citrate-dithionite for the reduction of molybdate-P. The absorbance measurement of P was made at 730nm. Absorbance measurement for all the analyses was performed using a Shimadzu UV-1700 spectrophotometer with a 1-cm quartz cell, and duplicates were measured for each sample. For the calibration and accuracy assessment, matrix-matched reagent blanks and standards were prepared. The calibration standard was made using Merck phosphate standard (1000 mg/L). The reactive P (P_{react}) is the sum of all non-detrital fractions

($P_{\text{react}} = P_{\text{bio}} + P_{\text{Fe}} + P_{\text{auth}} + P_{\text{org}}$) while the P_{total} represents sum of all five fractions. Duplicates were included in the extraction steps to monitor the repeatability of the extraction method. The estimated analytical precisions based on duplicate analyses of our samples were generally < 10%.

2.4. Chronology of the sediment cores

The chronology of the short cores was established using Accelerator Mass Spectrometer (AMS) ^{14}C dates of ~10 mg mixed planktonic foraminifera from >125 μm fraction of six samples (**Table 1**) with the facility at Inter-University Accelerator Centre (IUAC), Delhi. CALIB 8.1.0 online software program (Reimer et al., 2009) along with the MARINE20 dataset was used to calibrate the conventional ^{14}C dates to calendar years after applying a regional reservoir age correction (ΔR) of 356 for the western Bay of Bengal (Southon et al., 2002).

3. Results

The results of our study are shown in **Supplementary Table 1** and **Table 2**, and Figures 2 and 3. To better present them in the context of depositional environment, sediment cores were described as Palar basin cores (SPC5 and SPC7) and the Cauvery basin cores (SPC3 and SPC13). The C_{org} content in these sediments vary between 0.31 and 2 wt.% (**Fig. 2**) with an average of 1.01 wt.% (**Supplementary Table 2**). Higher C_{org} content is seen in Palar basin compared to the Cauvery basin. The C_{org} content does not show any prominent downcore decrease except at the station SPC13, where C_{org} content decreases from 1.16 wt.% at the surface to 0.41 wt.% at the bottom (**Fig. 2**). The CaCO_3 content ranges from 4.9 to 40.3 wt.% with an average of 17.1 wt.% (Fig. 2). Compared to Cauvery basin (SPC3 and SPC13), CaCO_3 content is relatively high in sediment cores SPC5 and SPC7 from the Palar basin. The CaCO_3 content increases with depth in core SPC5. N_{total} content decreases with sediment depth at all stations and varies between 0.032 and 0.164 wt.% (average 0.095 wt.%). The sediment core SPC3 has lower N_{total} content (average 0.037 wt.%) than at other stations (**Fig. 2**).

DIP concentration in the porewater varies between 4 and 32 $\mu\text{mol/L}$ with an average of 12.4 $\mu\text{mol/L}$ (**Fig. 3**). Downcore DIP profiles mostly show higher values at the surface with a gradual decrease with depth, with the decrease being more prominent in sediment cores SPC7 and SPC13. DIP concentration in SPC5 shows a rapid decrease at 3 cm depth after surface enrichment, followed by a gradual increase with depth up to 13 cm (**Fig. 3**). Bottom water DIP concentration varies between 0.65 and 2.72 $\mu\text{mol/L}$ and the lowest concentration was observed at SPC3 core location (**Table 2**).

P_{total} content in the cores ranges between 17.2 and 531 $\mu\text{mol/g}$ (Supplementary Table 1 and **Fig. 4**), with an average of 91 $\mu\text{mol/g}$. The highest values were found in core SPC7, in which the concentration varies between 112 and 531 $\mu\text{mol/g}$ (average 242 $\mu\text{mol/g}$). P_{bio} content in the present study ranges between 3.3 and 60.2 $\mu\text{mol/g}$, accounting for 9.5 to 46% of the P_{total} (**Fig. 5**), with a slight subsurface increase in cores SPC5 and SPC3. P_{bio} content is relatively high in core SPC7 and varies from 19 to 60.2 $\mu\text{mol/g}$ (Supplementary Table 1), averaging 34.5 $\mu\text{mol/g}$. The P_{Fe} concentrations are very low (average 10.5 $\mu\text{mol/g}$) and account for 11% (average) of the P_{total} . Downcore profiles of P_{Fe} content show great variation between stations. In SPC3, P_{Fe} content decreases with depth and accounts for 2.3-5.5 % of the P_{total} (**Fig. 5**). Relatively high P_{Fe} content is observed in core SPC7 (Supplementary Table 1) which accounts for 4.8-22.4% of the total.

The P_{auth} content varies from 1.2 to 221 $\mu\text{mol/g}$ and accounts for 4.7 - 49 % of the P_{total} . It is the major form of sedimentary P reservoir at SPC7 and SPC3 locations and accounts for 40 and 37% (average) of the P_{total} , respectively. No significant downcore trend is seen in P_{auth} , except for a slight increase with depth from 2.3 to 17.2 $\mu\text{mol/g}$ in SPC5. The P_{det} fraction represents the second-largest sedimentary P reservoir in the present study. P_{det} content varies between 3.5 and 173 $\mu\text{mol/g}$ (Supplementary Table 1) and accounts for 4.9 to 38 % of the P_{total} . The core SPC7 (Palar) has the highest P_{det} content, which ranges between 11.2 and 25 $\mu\text{mol/g}$.

The P_{org} content is very low, ranges between 1.55 and 24.98 $\mu\text{mol/g}$ (Supplementary Table 1) (with an average of 8.11 $\mu\text{mol/g}$) and constitutes ~12.6% (average) of the P_{total} . In core SPC5, P_{org} shows a gradual decrease from surface (11.7 $\mu\text{mol/g}$) to a depth of 6cm (6.4 $\mu\text{mol/g}$). The concentration is nearly similar until 20 cm before showing a gradual decrease again. SPC13 shows a gradual decrease of P_{org} with depth. At station SPC3, while the P_{org} content is low at the surface, it increases with depth. Compared to other cores, SPC7 does not show any prominent downcore trend of P_{org} with depth (Fig. 5) and accounts for only 7.7 % (average) of the P_{total} .

4. Discussion

4.1. Ages, sedimentation rates and depositional environment

The AMS ^{14}C derived dates are presented in **Table 1**. The ages are 7.313 kyr for the surface (2-3 cm) of sediment core SPC5 from the Palar basin, suggesting that the present-day sediment accumulation in this region is very low. At the same time, the bottom section of the core (25.5 cm) shows an age of ~10.99 kyr indicating comparatively higher sedimentation during early Holocene compared to the late Holocene. Similarly, ^{14}C ages of bottom section (18.5 cm) of the second core from the Palar basin (SPC-7) is 8.504 kyr. This reflects a shift in sedimentation in this region during

the early to mid-Holocene. The calculated sedimentation rate between two ^{14}C dated section of SPC 5 is 6.25 cm/kyr. The locations of cores SPC7 and SPC5 are in the outer shelf region and fall in the phosphorite-occurring zone (Vaz, 1995). Sub-bottom profiles in this region show the signature of sediment fills on the irregular hard acoustic basement (Susanth et al., 2021a). The sediment fills in the top unit vary across the outer shelf, with the presence of rock outcrops on the seafloor, conspicuous of an erosional surface. The lack of sediments above this unit indicates low sedimentation or erosional activity. Evidence from remote sensing studies from Resmi et al. (2017) shows the north-to-south shift in the paleochannels of Palar River, which might have influenced the sedimentation in the offshore Basin. This study of Resmi et.al. (2017) identified paleochannels located in the northern part of the present-day river, indicating migration of river course towards the south during the mid-to Late Holocene (4.83 to 1.88 ka years ago; Fig. 1).

However, further south of the sample locations of SPC7 and SPC5, the continental slope is characterized by Palar Canyon System (Susanth et al., 2021b). The twenty deeply incised canyons that indent the shelf edge act as a conduit for sediments transport to deeper waters. Since the present-day active channel of the river influences the activity of Palar canyons, this part of the shelf is expected to have high sedimentation compared to the north, and this is evident from the study of our samples. The north-to-south migration of the Palar River could be the reason for the shift in sedimentation in this region. Apart from the shift in sedimentation in this area, the missing top section also suggests the removal of sediments in this region. This could be due to the erosion/winnowing of sediments. Such records of erosional and winnowing activity off- Chennai region was reported earlier (Symphonia and Nathan, 2018). Past erosional activity during the lowered sea level stands was also reported in a sedimentary record off Chennai (Sebastian et al., 2023). Slope failure or strong bottom water currents can also lead to erosion. Several reasons such as topographic gradients, regional fault system, diapirism, fluid/gas movement, and neotectonic activity were attributed for the slumping and sliding features noticed in upper slope sediments in the Krishna Godavari offshore basin(Ramprasad et al., 2011).

The age model of the core SPC-13 from the Cauvery basin indicates ages of 2.124 kyr for the top section (2-3cm) and 2.682 kyr for the bottom section (26-27cm) we retrieved. The bottom section of the second core (SPC3) in the region shows a comparable age of 2.44 kyr. The estimated sedimentation rate in the Cauvery basin core is ~43.9 cm/kyr, indicating that the sedimentation in this area is significantly high compared to the Palar Basin for the time the core has covered. The sedimentation rates thus observed indicate that the sedimentation gradually increases from north to south which corroborates well with the shelf-slope morphology (Susanth et al., 2021b, 2021a). The

higher sedimentation rate in Cauvery Basin is attributed to the high sediment influx from the Cauvery river, which has sculpted prominent shelf indenting canyons in gentle slopes, and has created sinuous channels carrying 'mass transport complexes' towards deeper waters (Bastia et al., 2011). However, the ^{14}C ages of the top section of the sediment cores from both areas indicate that very recent sediments are possibly lost which could be due to erosion and resuspension of sediments in this region but with a major loss in area off Palar.

4.2. Nature and degradation of organic matter

Molar $\text{C}_{\text{org}}/\text{N}$ ratio can be used to characterize the source of organic matter in sediments where freshly precipitated organic matter of marine origin has a ratio of 6 - 9 (Perdue and Koprivnjak, 2007; Prahl et al., 1994, 1980), while the terrestrial vascular plants have molar $\text{C}_{\text{org}}/\text{N}$ ratio of 12 - 14 or above (Gearing, 1988; Jia and Peng, 2003). The molar $\text{C}_{\text{org}}/\text{N}$ ratio in the present study with an average of 12.43 (**Fig. 3**) indicates that most of the organic matter (OM) in this area is terrigenous in nature, which is consistent with the stable isotope-based findings of dominant allochthonous OM in the eastern continental margin of India (Krishna et al., 2013). The presence of terrestrially derived organic matter in sediments of BoB is not surprising as it receives large lithogenic flux by rivers draining from the Himalayas and Peninsular India (Bird et al., 2008; Tripathy et al., 2014). The annual riverine supply of sediment to BoB is about 13.5×10^8 tons which accounts for ~ 8% of the global value (Milliman and Syvitski, 1992; Tripathy et al., 2014). A high molar $\text{C}_{\text{org}}/\text{N}$ ratio (average 16.5) is observed in Palar core SPC7 (**Fig. 5**) suggesting higher terrestrial derived organic carbon input at this site than at other stations. High molar $\text{C}_{\text{org}}/\text{N}$ ratio at SPC7 is consistent with the high P_{det} content at this site, while the lower ratios (average 9) in core SPC13 indicate organic matter of marine origin.

Freshwater-induced stratification and weak wind forces over the BoB together restrict the vertical mixing to a shallow depth and inhibit the nutrient transport below the mixed layer resulting in low productivity in the BoB (Kumar et al., 2002). Due to the low productivity, marine-derived organic matter in BoB sediments is low. The downcore decrease of C_{org} and P_{org} contents at the SPC13 station indicates the degradation of organic matter and release of P into the porewater. However, no such degradation is observed at the other sampling sites which are dominated by terrestrial organic matter. Marine organic matter is more reactive than terrestrial organic matter and undergoes efficient remineralization (Burdige, 2005).

Molar $\text{C}_{\text{org}}/\text{P}_{\text{org}}$ and $\text{C}_{\text{org}}/\text{P}_{\text{react}}$ ratios in marine sediments can also be used to understand the source of organic matter and its behavior in sediments (Ruttenberg, 2003; Kraal et al., 2012; Yang et

al., 2017). The typical C_{org}/P_{org} ratio of fresh marine phytoplankton samples is around 106 (Redfield, 1963), while terrestrial vascular plants will have a high ratio of 800 to 2050 ((Likens et al., 1981; Simpson et al., 1977). The low molar C_{org}/P_{org} ratio (average 68) at the SPC7 site (**Fig. 3**) is similar to the river dominated coastal regimes of tropical Amazon shelf sediments (38-72) (Ruttenberg and Goñi, 1997) and East China Sea (<100) (Yang et al., 2017). This is probably due to the presence of refractory organic matter, enriched in P (van der Zee et al., 2002; Yang et al., 2017). This is also evident from the downcore profiles of C_{org} (**Fig. 2**) and P_{org} (**Fig. 4**), where the signatures of remineralization of organic matter with depth are not seen. Comparatively high C_{org}/P_{org} ratios at the SPC13 site suggest the degradation of organic matter and release of P. At station SPC5, a slight increase in C_{org}/P_{org} ratios from the surface to 10 cm down the core (**Fig. 3**) with a corresponding decrease in P_{org} (**Fig. 4**) is observed, which implies the preferential release of P relative to carbon. At all these sites, the sediments are overlain by oxygen-depleted water (**Table 2**). Preferential release of P from organic matter is more enhanced under the oxygen-depleted conditions (Ingall and Jahnke, 1994). The molar C_{org}/P_{react} ratio is an indicator of P burial in sediments (Kraal et al., 2012) and is a good tool for studying the fate of sedimentary P buried in sediments (Anderson et al., 2001). The low molar C_{org}/P_{react} ratio in the present study (**Fig. 5**) indicates that most of the sedimentary P phases are undergoing burial rather than regeneration.

Even though the P_{org} and C_{org} contents of BoB are comparable with Arabian Sea (Babu and Nath, 2005; Babu and Ramaswamy, 2017), organic matter degradation plays a minor role in the benthic porewater release of P in BoB. The high influx of organic matter in sediments resulting from monsoon-driven primary production and its degradation with depth make P_{org} a key factor controlling benthic phosphate release in the Arabian Sea sediments (Schenau and De Lange, 2001; Babu and Nath, 2005; Linsy et al., 2018b). Along with this, intense OMZ in Arabian Sea also enhances the preferential release of P relative to C_{org} (Babu and Nath, 2005; Linsy et al., 2018b) since the preferential release of P from organic matter is most extensive under oxygen-depleted conditions (Ingall and Jhanke, 1994). Though the bottom water DO values at the sites studied here are low, the high terrestrially derived fluvial sediment fluxes seem to hinder the redistribution of sedimentary P phases by enabling the burial rather than regeneration. Thus in studied region, the benthic regeneration of P is limited due to the enhanced preservation of organic matter.

4.3. Authigenic apatite formation

Formation of P_{auth} is the major pathway through which the reactive P is buried in the sediments. The sink switching of P from the labile to the authigenic phase is more common in upwelling areas characterized by oxygen-depleted water (Ruttenberg and Berner, 1993; Anderson et al., 2001;

Ruttenberg, 2003). Present-day carbonate fluorapatite (CFA) formation at the expense of organic matter degradation was also reported in the non-upwelling areas such as the Long Island Sound and the shallow Mississippi Delta (Ruttenberg and Berner, 1993). In the present study, the highest P_{auth} and P_{Total} contents are found at the SPC7 station (Palar) but without any significant downcore changes in other reactive phases (**Fig. 4**). Porewater profile of SPC7 shows decrease of DIP concentration close to the surface (**Fig. 3**), but a corresponding increase of P_{auth} is not observed, indicating that porewater is not used up for the CFA formation atleast recently. Downcore P_{auth} profile of SPC7 is very similar to the P_{det} profile, suggesting most of P_{auth} fraction is detrital in origin. As mentioned before, SPC7 (Palar) is located in the continental margin where the occurrence of phosphorites were reported earlier (Vaz et al., 1999; Rao et al., 2002, 2000). This area is characterized by weak upwelling and floored by relict carbonate sediments (Vaz et al., 1999) with a sandy to silty texture (Sebastian et al., 2019). Sediment texture and density data of the present study (**Fig. S1**) also suggest the presence of coarse-grained sediments at SPC7 sampling location. Among the two sediment cores of the Palar Basin, P_{auth} content is high at SPC7 compared to SPC5, as the former is situated on the shelf marginal depressions in which the abundance of phosphorites has been reported earlier (Rao et al., 2002). SPC5 was collected a little away which possibly receives less terrigenous materials than SPC7. The textural data reported by Sebastian et al. (2019) for the core-top samples of SPC7 (sand;11.47%, silt;32.8% ,clay:55.73%) and SPC-5 (sand:50.38%, silt:16.14%, clay:33.48%) are varying significantly suggesting the difference in the depositional regimes. This is also evident from the multi-sensor core logger derived volume magnetic susceptibility data (Sebastian et al., 2019) which shows high values for SPC 7 compared to SPC 5 suggesting more detrital contribution at SPC-7 location (**Fig. S1**).

P_{auth} content is low at the SPC13 station (Cauvery basin), which is dominated by P_{det} . The core SPC13 was collected from the margin off the Kollidam River mouth and the riverine sediment input may have curtailed the formation of authigenic apatite. Low P_{auth} at SPC 13 is similar to estuaries that get substantial river inflow, where P_{det} is dominant, and with low P_{auth} content (Hou et al., 2009; Liang et al., 2021; Meng et al., 2014). At the adjoining sampling site SPC3 (Cauvery), P_{auth} content is predominant, while P_{det} is the second largest fraction. However, the decrease of other reactive phases is not observed at this site (core SPC3). This suggests that most of the P_{auth} content at SPC3 is also detrital in origin and present-day phosphogenesis is not taking place in this area. The P_{Total} content of both SPC3 (average 23.2 $\mu\text{mol/g}$) and SPC13 (21.6 $\mu\text{mol/g}$) are nearly similar. High sedimentation rate in the Cauvery basin could be one of the reasons for the absence of phosphogenesis in the studied samples. High sedimentation rate leads to the rapid burial of reactive P

and limits the sink-switching of P from the labile to authigenic phase (Acharya et al., 2016; Filippelli, 1997).

High detrital input and relatively low productivity in the area limits the release of P to the porewater and impede the in-situ formation of authigenic apatite in the area. Two prerequisites that are needed for authigenic apatite formation are the saturation of phosphate in porewater and sedimentary condition which favors the nucleation of phosphate in the porewater (Schenau et al., 2005; Van Cappellen and Berner, 1988; van der Zee et al., 2002). But, unfavorable conditions like the low input of reactive P and their subsequent rapid burial by ballasting effect seem to inhibit the sink switching of P from labile to authigenic phases in western BoB.

4.4. Burial of Phosphorus in the BoB Sediments

In addition to exchangeable or loosely sorbed, carbonate-related P, the P_{bio} fraction recovered here also would contain P from biogenic apatite/hydroxyapatite. Burial of fish debris consisting of hydroxyapatite is the potential source of reactive P to the sediments (Schenau and De Lange, 2000; Suess, 1981). Dissolution of fish debris enhances the benthic porewater phosphate fluxes in highly productive areas and may lead to P_{auth} formation (Linsy et al., 2018b; Schenau and De Lange, 2001; Suess, 1981). The fish debris dissolution may release phosphorus into the overlying water and enhance biological productivity (Schenau and De Lange, 2001). P_{bio} content is relatively low at SPC13 and SPC3 stations (both Cauvery). The productivity of the Bay of Bengal is relatively low (89.4 - 220.7 mg C m⁻² d⁻¹ - Madhupratap et al., 2003) compared to the Arabian Sea (770 - 1782 mg C m⁻² d⁻¹ - Prasanna Kumar et al., 2001). Lower productivity is expected to lower the fish production in BoB, leading to a reduced burial rate of P_{bio} . The regeneration of P at the expense of biogenic apatite dissolution is indicated by a decrease in P_{bio} with depth and an accompanying rise in porewater DIP as clearly noticed in the Eastern Arabian Sea (Linsy et al., 2018b). However, no significant downcore decrease of P_{bio} is observed (**Fig. 4**) in the present studied cores, suggesting the preservation of P_{bio} with depth.

P_{bio} phase extracted here can also contain carbonate-associated P and exchangeable P (see Schenau and De Lange, 2000; Babu and Nath, 2005). Relatively high P_{bio} at the site SPC5 and SPC7 (Palar basin) could be mainly due to the carbonate-associated P. Sediments in the phosphatic zone are comprised of relict carbonate sediments (Vaz et al., 1999; Rao et al., 2000) and the variation of P_{bio} is very similar to other phases implying a common source. CaCO₃ content at SPC 5 (average 23.7 wt.%) and SPC 7 (average 32 wt.%) stations (Palar) is relatively high compared to the other two stations, SPC 3 (average 7.6 wt.%) and SPC 13 (average 6 wt.%) in the Cauvery basin

(**Supplementary Table 2**). All these results suggest that dissolution of P_{bio} is playing a weak role in the benthic regeneration of P in BoB, where most of P_{bio} is undergoing burial rather than regeneration. This observation is unlike that of the Arabian Sea, where P_{bio} is the dominant sedimentary P phase, and its dissolution significantly enhance the benthic fluxes of phosphate (Schenau and De Lange, 2001, Linsy et al., 2018b).

Iron oxides have a high affinity for P and scavenge dissolved P from water columns and sediments in oxic conditions (Slomp et al., 1996). But under reducing conditions, iron oxyhydroxides undergo reduction and release phosphate to the porewater/overlying water, thereby enhancing the benthic porewater fluxes and facilitate the P_{auth} formation in sediments (e.g., Slomp et al., 1996; Filippelli, 2001). Based on near bottom water oxygen concentration (**Table 2**) and classification of oxygenation conditions by Naqvi et al. (2010), the bottom waters at all four stations of the present study fall in hypoxic category ($4.46 < O_2 \leq 62.49 \mu\text{M}$). Accordingly P_{Fe} constitutes only a minor fraction of the total P in the present study (average 12% of the P_{total}), and except at SPC7 station, the values are comparable with the previously reported values in the BoB (Babu and Ramaswamy, 2017). Highest P_{Fe} contents are found in core SPC7 (Palar), which is dominated by the detrital input. Other P fractions are also high at this station, and the high P_{Fe} content may be due to the difference in depositional flux. In this study, even under reducing conditions, P_{Fe} content at SPC5 and SPC7 does not show a prominent downcore decrease with depth (**Fig. 4**), and distinct downcore peaks are exactly matching with the P_{det} variation indicating the change in the deposition. The majority of the iron oxides brought by detrital supply are more crystalline (Wang et al., 2019; Zhu et al., 2012), and as crystallinity increases, the adsorption capacity of the Fe-oxide declines (Ruttenberg and Sulak, 2011). Most of these stations are dominated by detrital input, which makes P_{Fe} a minor contributor to the P_{total} (**Fig. 5**).

Despite the OMZ, denitrification in the water column is not found to occur in BoB (Madhupratap et al., 2003; Rao et al., 1994; Bristow et al., 2017). The incomplete oxidation of organic matter and their rapid removal by ballasting effect results in a low bacterial respiration rate in the BoB (Naqvi et al., 1996). Low bacterial respiration is attributed as the reason for the absence of denitrification in the BoB compared to the Arabian Sea (Rao et al., 1994; Naqvi et al., 1996; Sarma et al., 2013). Due to the low bacterial respiration, microbial reduction of iron oxyhydroxides is also low in BoB, making redox cycling of iron only a minor player in the P geochemistry of BoB sediments. Along with this, the low adsorption capacity of terrigenously derived iron oxides also makes P_{Fe} a minor sedimentary phase. Thus, the findings of the present study suggest that Fe redox cycling plays only a limited role in the P geochemistry in this area. However, it contrasts with a

previous work by Babu and Ramaswamy (2017) where they found higher P_{Fe} content in the deeper sediments (500 to 1500m depths which are beyond the OMZ) of BoB compared to shallower sediments they studied, and were attributed by them to strong diagenetic iron-oxide cycling. This is typical of oxic sediments as the iron oxides are excellent hosts of P in oxic conditions (Linsy et al., 2018a).

4.5. Porewater profiles, benthic porewater fluxes, and burial efficiency

As mentioned before, phosphorus limitation severely limits the N_2 fixation and primary productivity in the Bay of Bengal (Rao et al., 2021; Sarma et al., 2020). Adsorption of phosphorus on the suspended particulate matter and their rapid removal from the water column decreases the primary productivity by 1 to 2% in the Bay of Bengal (Rao et al., 2021; Sarma, 2022; Sarma et al., 2020). Considering the importance of limitation of P in the water column, we have calculated the diffusive flux of phosphate at the sediment-water interface (see Linsy et al., 2018b for the method followed based on Fick's law of diffusion), from the porewater and bottom water P data, to understand the exchange of P between sediment and water column. The estimated benthic flux in the study area indicates the release of P from sediments to the overlying water. The estimated benthic fluxes of porewater in this area (**Table 2**) are comparable with the previously reported values in the Arabian Sea (Linsy et al., 2018b). High benthic fluxes of phosphate in the Arabian Sea were mainly attributed to the dissolution of fish debris and preferential release of P from organic matter (Schenau and De Lange, 2001; Linsy et al., 2018b); whereas high P fluxes at the BoB sediments originate from substantially high porewater phosphate concentration at the sediment-water interface (**Fig. 3**). Due to low productivity, P_{bio} and P_{org} content in the BoB sediments are very low and along with this, high sedimentation rate also limits the release of P. The flux of particulate organic and inorganic P in the Indian Ocean through river input is 0.2 and 1.5×10^6 tons per year respectively (Ramesh et al., 1995). The BoB receives a large amount of phosphate (0.08 ± 0.02 Tg yr^{-1}) than the Arabian Sea (0.03 ± 0.007 Tg yr^{-1}) through river input (Krishna et al., 2016). Despite the low benthic release of P through organic matter degradation and dissolution of P_{bio} , high benthic porewater phosphate fluxes at the sediment-water interface in BoB are mainly due to high particulate phosphate supply through river input. Relatively high benthic fluxes are seen at SPC7 and SPC3 sites (Table 2) which receive high terrigenous input compared to the other two stations.

The porewater DIP profiles (**Fig. 3**) show the highest values at the surface except at SPC5 station (Palar). High DIP concentrations at the surface of the sediments are attributed to the release of P from easily degradable organic matter deposited at the sediment-water interface. At core site SPC5, DIP concentration increases with depth with a corresponding decrease of P_{org} content

indicating the preferential release of P from organic matter. At stations SPC7 (Palar) and SPC13 (Cauvery), depletion of porewater DIP with depth is observed (**Fig. 3**), but a corresponding increase of P_{auth} content (**Fig. 4**) is not found. In-situ formation of authigenic apatite is not reflected in the downcore data as the subsurface changes in P_{auth} corresponds to changes in P_{det} . This is different to the Eastern Arabian Sea, where phosphogenesis has been documented, a subsurface decrease in porewater P was noticed which corresponded to an increase in P_{auth} (Fig. S1) implying that the porewater P is being used up in formation of authigenic apatite (Linsy et al., 2018b). Downcore porewater profiles in the BoB sediment cores, studied here, show no such subsurface change indicative of utilization of dissolved P of porewater. Burial efficiency of phosphorus in the sediments was calculated to understand the extent of regeneration/burial in the study area. Phosphorus burial efficiency in sediments was calculated using P mass accumulation rate (PAR) and benthic flux of phosphate (Jp). The formula is

$$\text{Burial Efficiency} = 100 \times \text{PAR} / (\text{PAR} + \text{JP}) \text{ (Fang et al., 2007).}$$

The estimated burial efficiency of P ranges between 12.6 and 48.2% for the period of sedimentation. High burial efficiency was observed in Cauvery basin (48.2%) which is likely due to the high sediment accumulation rate in this area. The burial efficiency in this area is relatively higher than the samples from the eastern Arabian Sea where phosphogenesis was reported (Linsy et al., 2018b) but comparable with Oman and Pakistan margin sediments (Schenau and De Lange, 2001). Anoxic sediments in the Black Sea are estimated to have a burial efficiency of about 27% (Dijkstra et al., 2018), which is comparable with the Palar Basin but lower than that of the Cauvery Basin (present study). The burial efficiency of the Palar basin is also comparable to that found in the Central Baltic Sea (0.2-12%) (Viktorsson et al., 2013) but substantially lower than that of the shelf sediments of the East China Sea (90%) (Fang et al., 2007). In the Palar basin, burial efficiency is relatively higher in core SPC7 than in SPC5, which is attributed to the accumulation of high amount of P_{det} which is resistant to regeneration during diagenetic processes. In summary, P geochemistry in BoB is guided by different depositional conditions prevalent here.

5. Conclusions

Downcore porewater profiles and solid phase P speciation data indicate that sedimentary cycling of P in BoB is mostly regulated by the input of lithogenic fluxes in the area. The low decomposition rate of organic matter in the water column as well as in sediments and the abundance of terrestrial organic matter make P_{org} a minor player in P cycling. Unfavorable conditions such as low input of reactive P, high input of non-reactive P through river runoff and their rapid burial by

ballast effect seems to inhibit the sink switching of P from labile to authigenic phase. Thus, most of the P_{auth} extracted here is terrigenous in origin and unlike in the eastern Arabian Sea, no present day phosphogenesis signatures are visible. P_{Fe} plays only a minor role in the benthic regeneration of P in the present study due to the low bacterial respiration. This limits the microbial reduction of iron oxyhydroxides which, in combination with a low adsorption capacity of terrigenously derived iron oxide, make the redox cycling of iron a weak player in the area. Results of the present study suggest that the recent sedimentation in Palar basin is relatively low due to the migration of river course towards the south during the mid to Late Holocene. The burial efficiency of P is relatively high in the Cauvery basin owing to the high sediment accumulation rate. The core tops of both the sites, however, show older age likely due to the erosion/winnowing.

Acknowledgments

The authors thank all the shipboard participants who helped during the sampling and operations, Director, CSIR-NIO, for permission to publish and for providing the ship time, Dr. Prakah Babu for TC and TIC analyses, E. Prajina; Lakulish Sharma for P speciation analyses and Dr. N.H Khadge for salary support from GAP-2128 to PL. Authors are thankful to IUAC for extending AMS facility for ^{14}C funded by Ministry of Earth Science (MoES), Govt. of India with reference numbers MoES/16/07/11(i)-RDEAS and MoES/P.O.(Seismic)8(09)-Geochron/2012. We are grateful to Mr. S. Susanth for generating the overview map. Thanks to Editor Dr. Adina Paytan and the anonymous reviewer for their thorough reviews. All the analytical expenses were met from Project PSC-0106 to fulfill the objectives of CSIR XII Plan Project GEOSINKS. This is NIO Contribution No. xxxx.

Author statement

Conceptualization - PL and BNN, methodology- PL, validation-PL and BNN, formal analysis-PL, EP, SL, DR, SJ, AK, BR and SP, investigation-PL and BNN, data curation-PL, BNN, MBL, writing—original draft preparation-PL, writing- review and editing – PL, BNN, MBL and TS, visualization- LP, TS, resources-BNN, supervision-BNN, project administration and funding acquisition-BNN

Declaration of Competing Interest

The authors declare that they have no known competing financial interests or personal relationships that could have appeared to influence the work reported in this paper.

Data availability

Full data made available as a supplementary file.

References

- Acharya, S.S., Panigrahi, M.K., Kurian, J., Gupta, A.K., Tripathy, S., 2016. Speciation of phosphorus in the continental shelf sediments in the Eastern Arabian Sea. *Cont. Shelf Res.* 115, 65–75. <https://doi.org/10.1016/j.csr.2016.01.005>
- Anderson, L.D., Delaney, M.L., Faul, K.L., 2001. Carbon to phosphorus ratios in sediments: Implications for nutrient cycling. *Global Biogeochem. Cycles* 15, 65–79. <https://doi.org/10.1029/2000GB001270>
- Babu, C.P., Nath, B.N., 2005. Processes controlling forms of phosphorus in surficial sediments from the eastern Arabian Sea impinged by varying bottom water oxygenation conditions. *Deep. Res. Part II Top. Stud. Oceanogr.* 52, 1965–1980. <https://doi.org/10.1016/j.dsr2.2005.06.004>
- Babu, C.P., Ramaswamy, V., 2017. Phosphorus Accumulation Associated with Intense Diagenetic Metal-Oxide Cycling in Sediments along the Eastern Continental Margin of India. *Curr. Sci.* 113, 473–478. <https://doi.org/10.18520/CS/V113/I03/473-478>
- Bastia, R., Radhakrishna, M., Nayak, S., 2011. Identification and characterization of marine geohazards in the deep water eastern offshore of India: Constraints from multibeam bathymetry, side scan sonar and 3D high-resolution seismic data. *Nat. Hazards* 57, 107–120. <https://doi.org/10.1007/S11069-010-9625-3>
- Bird, M.I., Robinson, R.A.J., Oo, N.W., Aye, M.M., Lu, X.X., Higgitt, D.L., Swe, A., Tun, T., Lhaing Win, S., Sandar Aye, K., Mi, K., Win, M., Hoey, T.B., 2008. A preliminary estimate of organic carbon transport by the Ayeyarwady (Irrawaddy) and Thanlwin (Salween) Rivers of Myanmar. *Quat. Int.* 186, 113--122. <https://doi.org/10.1016/j.quaint.2007.08.003>
- Burdige, D.J., 2005. Burial of terrestrial organic matter in marine sediments: A re-assessment. *Global Biogeochem. Cycles* 19, n/a-n/a. <https://doi.org/10.1029/2004GB002368>
- Carritt, D., Carpenter, J., 1966. Comparison and evaluation of currently employed modifications of the Winkler method for determining dissolved oxygen in seawater; A NASCO report. *J. Mar. Res.* 24.
- Compton, J., Mallinson, D., Glenn, C.R., Filippelli, G., Follmi, K., Shields, G., Zanin, Y., 2000. Variations in the global phosphorus cycle. *Mar. Authigenes. From Glob. to Microb.* 21–33. <https://doi.org/10.2110/pec.00.66.0021>
- Compton, J.S., Bergh, E.W., 2016. Phosphorite deposits on the Namibian shelf. *Mar. Geol.* 380, 290–314. <https://doi.org/10.1016/j.margeo.2016.04.006>
- Datta, D.K., Gupta, L.P., Subramanian, V., 1999. Distribution of C, N and P in the sediments of the Ganges-Brahmaputra-Meghna river system in the Bengal basin. *Org. Geochem.* 30, 75–82. [https://doi.org/10.1016/S0146-6380\(98\)00203-4](https://doi.org/10.1016/S0146-6380(98)00203-4)

- Dijkstra, N., Kraal, P., Séguret, M.J.M., Flores, M.R., Gonzalez, S., Rijkenberg, M.J.A., Slomp, C.P., 2018. Phosphorus dynamics in and below the redoxcline in the Black Sea and implications for phosphorus burial. *Geochim. Cosmochim. Acta* 222, 685–703. <https://doi.org/10.1016/j.gca.2017.11.016>
- Fang, T.H., Chen, J.L., Huh, C.A., 2007. Sedimentary phosphorus species and sedimentation flux in the East China Sea. *Cont. Shelf Res.* 27, 1465–1476. <https://doi.org/10.1016/j.csr.2007.01.011>
- Filippelli, G.M., 2011. Phosphate rock formation and marine phosphorus geochemistry: The deep time perspective. *Chemosphere* 84, 759–766. <https://doi.org/10.1016/j.chemosphere.2011.02.019>
- Filippelli, G.M., 2001. Carbon and phosphorus cycling in anoxic sediments of the Saanich Inlet, British Columbia. *Mar. Geol.* 174, 307–321. [https://doi.org/10.1016/S0025-3227\(00\)00157-2](https://doi.org/10.1016/S0025-3227(00)00157-2)
- Filippelli, G.M., 1997. Controls on phosphorus concentration and accumulation in oceanic sediments. *Mar. Geol.* 139, 231–240. [https://doi.org/10.1016/S0025-3227\(96\)00113-2](https://doi.org/10.1016/S0025-3227(96)00113-2)
- Gearing, J.N., 1988. The use of stable isotope ratios for tracing the nearshore-offshore exchange of organic matter, in: *Coastal-Offshore Ecosystem Interactions*. Springer, Berlin, Heidelberg, pp. 69–101. https://doi.org/10.1007/978-3-642-52452-3_4
- Grasshoff, K., Ehrhardt, M., Kremling, K., 1983. *Methods of seawater analysis*, 419 pp, Verlag Chemie, New York.
- Holeman, O.N., 1968. *The Sediment Yield of Major Rivers the World*. *Water Resour. Res.* 4.
- Holland, H.D., 1978. *The chemistry of the atmosphere and oceans - (v. 1)*.
- Hou, L.J., Liu, M., Yang, Y., Ou, D.N., Lin, X., Chen, H., Xu, S.Y., 2009. Phosphorus speciation and availability in intertidal sediments of the Yangtze Estuary, China. *Appl. Geochemistry* 24, 120–128. <https://doi.org/10.1016/j.apgeochem.2008.11.008>
- Howarth, R.W., Jensen, H.S., Marino, R., Postma, H., 1995. *Transport to and Processing of P in Near-Shore and Oceanic Waters*. Scope (Kalamazoo).
- Ingall, E., Jahnke, R., 1994. Evidence for enhanced phosphorus regeneration from marine sediments overlain by oxygen depleted waters. *Geochim. Cosmochim. Acta* 58, 2571–2575. [https://doi.org/10.1016/0016-7037\(94\)90033-7](https://doi.org/10.1016/0016-7037(94)90033-7)
- Ittekkot, V., Nair, R.R., Honjo, S., Ramaswamy, V., Bartsch, M., Manganini, S., Desai, B.N., 1991. Enhanced particle fluxes in Bay of Bengal induced by injection of fresh water. *Nature* 351, 385–387. <https://doi.org/10.1038/351385a0>
- Jia, G., Peng, P., 2003. Temporal and spatial variations in signatures of sedimented organic matter in Lingding Bay (Pearl estuary), southern China. *Mar. Chem.* 82, 47–54. [https://doi.org/10.1016/S0304-4203\(03\)00050-1](https://doi.org/10.1016/S0304-4203(03)00050-1)
- Kraal, P., Slomp, C.P., Reed, D.C., Reichart, G.J., Poulton, S.W., 2012. Sedimentary phosphorus and iron cycling in and below the oxygen minimum zone of the northern Arabian Sea. *Biogeosciences* 9, 2603–2624. <https://doi.org/10.5194/bg-9-2603-2012>

- Krishnan, M.S., 1982. Geology of India and Burma.
- Kumar, P.S., Muraleedharan, P.M., Prasad, T.G., Gauns, M., Ramaiah, N., de Souza, S.N., Sardesai, S., Madhupratap, M., 2002. Why is the Bay of Bengal less productive during summer monsoon compared to the Arabian Sea? *Geophys. Res. Lett.* 29, 88-1-88-4. <https://doi.org/10.1029/2002GL016013>
- Liang, B., Peng, S., Xu, W., Xiong, H., Zheng, T., 2021. Distribution and speciation of phosphorus in surface sediments of the intertidal zone in the yellow river delta. *IOP Conf. Ser. Earth Environ. Sci.* 621. <https://doi.org/10.1088/1755-1315/621/1/012091>
- Likens, G.E., Bormann, F.H., Johnson, N.M., 1981. Interactions Between Major Biogeochemical Cycles in Terrestrial Ecosystems, in: *Some Perspectives of the Major Biogeochemical Cycles*. Wiley New York, pp. 93–112.
- Linsy, P., Nagender Nath, B., Mascarenhas-Pereira, M.B.L., Chauhan, T., Sebastian, T., Babu, C.P., Kurian, S., Miriyala, P., Kazip, A., Borole, D.V., Khadge, N.H., 2018a. Distribution and Diagenesis of Phosphorus in the Deep-Sea Sediments of the Central Indian Basin. *J. Geophys. Res. Ocean.* <https://doi.org/10.1029/2018JC014386>
- Linsy, P., Nagender Nath, B., Mascarenhas-Pereira, M.B.L., Vinitha, P.V., Ray, D., Prakash Babu, C., Ramalingeswara Rao, B., Kazip, A., Sebastian, T., Kocherla, M., Miriyala, P., 2018b. Benthic cycling of phosphorus in the Eastern Arabian Sea: Evidence of present day phosphogenesis. *Mar. Chem.* 199, 53–66. <https://doi.org/10.1016/j.marchem.2018.01.007>
- Madhupratap, M., Gauns, M., Ramaiah, N., Prasanna Kumar, S., Muraleedharan, P.M., De Sousa, S.N., Sardesai, S., Muraleedharan, U., 2003. Biogeochemistry of the Bay of Bengal: Physical, chemical and primary productivity characteristics of the central and western Bay of Bengal during summer monsoon 2001. *Deep. Res. Part II Top. Stud. Oceanogr.* 50, 881–896. [https://doi.org/10.1016/S0967-0645\(02\)00611-2](https://doi.org/10.1016/S0967-0645(02)00611-2)
- Meng, J., Yao, P., Yu, Z., Bianchi, T.S., Zhao, B., Pan, H., Li, D., 2014. Speciation, bioavailability and preservation of phosphorus in surface sediments of the Changjiang Estuary and adjacent East China Sea inner shelf. *Estuar. Coast. Shelf Sci.* 144, 27–38. <https://doi.org/10.1016/j.ecss.2014.04.015>
- Milliman, J.D., Meade, R.H., 1983. World-Wide Delivery of River Sediment to the Oceans. *J. Geol.* 91, 1–21. <https://doi.org/10.1086/628741>
- Milliman, J.D., Syvitski, J.P., 1992. Geomorphic/tectonic control of sediment discharge to the ocean: the importance of small mountainous rivers. *J. Geol.* 100, 525–544.
- Mohanty, A.K., Bramha, S.N., Satpathy, K.K., Padhi, R.K., Panigrahi, S.N., Samantara, M.K., 2018. Geochemical distribution of forms of phosphorus in marine sediment of Bay of Bengal , southeast coast of India. *Indian J. Geo-Marine Sci.* 47, 1132–1141.
- Naqvi, S.W.A., Shailaja, M.S., Dileep Kumar, M., Sen Gupta, R., 1996. Respiration rates in subsurface waters of the northern Indian Ocean: evidence for low decomposition rates of organic matter within the water column in the Bay of Bengal. *Deep Sea Res. Part II Top. Stud. Oceanogr.* 43, 73–81. [https://doi.org/10.1016/0967-0645\(95\)00080-1](https://doi.org/10.1016/0967-0645(95)00080-1)

- Naqvi, S.W.A.A., Bange, H.W., Fariñas, L., Monteiro, P.M.S.S., Scranton, M.I., Zhang, J., 2010. Marine hypoxia/anoxia as a source of CH₄ and N₂O. *Biogeosciences* 7, 2159–2190. <https://doi.org/10.5194/bg-7-2159-2010>
- Narasimha Chari, M. V., Sahu, J.N., Banerjee, B., Zutshi, P.L., Chandra, K., 1995. Evolution of the Cauvery basin, India from subsidence modelling. *Mar. Pet. Geol.* 12, 667–675. [https://doi.org/10.1016/0264-8172\(95\)98091-I](https://doi.org/10.1016/0264-8172(95)98091-I)
- Perdue, E., Koprivnjak, J., 2007. Using the C/N ratio to estimate terrigenous inputs of organic matter to aquatic environments. *Estuar. Coast. Shelf Sci.* 73, 65–72. <https://doi.org/10.1016/j.ecss.2006.12.021>
- Prahl, F., Bennett, J., Carpenter, R., 1980. The early diagenesis of aliphatic hydrocarbons and organic matter in sedimentary particulates from Dabob Bay, Washington. *Geochim. Cosmochim. Acta* 44, 1967–1976. [https://doi.org/10.1016/0016-7037\(80\)90196-9](https://doi.org/10.1016/0016-7037(80)90196-9)
- Prahl, F., Ertel, J., Goni, M., Sparrow, M., Eversmeyer, B., 1994. Terrestrial organic carbon contributions to sediments on the Washington margin. *Geochim. Cosmochim. Acta* 58, 3035–3048.
- Prasanna Kumar, S., Ramaiah, N., Gauns, M., Sarma, V.V.S.S., Muraleedharan, P.M., Raghukumar, S., Dileep Kumar, M., Madhupratap, M., 2001. Physical forcing of biological productivity in the Northern Arabian Sea during the Northeast Monsoon. *Deep Sea Res. Part II Top. Stud. Oceanogr.* 48, 1115–1126. [https://doi.org/10.1016/S0967-0645\(00\)00133-8](https://doi.org/10.1016/S0967-0645(00)00133-8)
- Ramesh, R., Purvaja, G.R., Subramanian, V., 1995. Carbon and phosphorus transport by the major Indian rivers. *J. Biogeogr.* 22, 409–415. <https://doi.org/10.2307/2845937>
- Ramprasad, T., Dewangan, P., Ramana, M. V, Mazumdar, A., Karisiddaiah, S.M., Ramya, E.R., Sriram, G., 2011. Evidence of slumping/sliding in KrishnaeGodavari offshore basin due to gas/fluid movements. *Mar. Pet. Geol.* 28, 1806–1816. <https://doi.org/10.1016/j.marpetgeo.2011.02.007>
- Rangaraju, M., Agrawal, A., Prabhakar, K., 1993. Structural styles, evolutionary model and hydrocarbon habitat, Cauvery and palar basins, proceedings of second seminar on petroliferous Basins of India. *Tectono-Stratigraphy-I* 371, e388.
- Rao, C.K., Naqvi, S.W., Kumar, M.D., Varaprasad, S.J., Jayakumar, D.A., George, M.D., Singbal, S.Y., 1994. Hydrochemistry of the Bay of Bengal: possible reasons for a different water-column cycling of carbon and nitrogen from the Arabian Sea. *Mar. Chem.* 47, 279–290. [https://doi.org/10.1016/0304-4203\(94\)90026-4](https://doi.org/10.1016/0304-4203(94)90026-4)
- Rao, D.N., Ghosh, V.R.D., Sam, P., Yadav, K., Sarma, V.V.S.S., 2021. Phosphate removal through adsorption on suspended matter in the Bay of Bengal: Possible implications to primary production. *J. Earth Syst. Sci.* 130, 1–16. <https://doi.org/10.1007/S12040-020-01524-8/FIGURES/9>
- Rao, V., Kessarkar, P., 2001. Geomorphology and geology of the Bay of Bengal and the Andaman Sea, in: *The Indian Ocean: A Perspective*. Oxford and IBH New Delhi, pp. 817–868.

- Rao, V., Michard, A., Naqvi, S.W.A., Böttcher, M.E., Krishnaswamy, R., Thamban, M., Natarajan, R., Borole, D. V., 2002. Quaternary phosphorites off the southeast coast of India. *Chem. Geol.* 182, 483–502. [https://doi.org/10.1016/S0009-2541\(01\)00336-9](https://doi.org/10.1016/S0009-2541(01)00336-9)
- Rao, V. P., Rao, K. M., Raju, D.S.N., 2000. Quaternary Phosphorites from the Continental Margin Off Chennai, Southeast India: Analogs of Ancient Phosphate Stromatolites. *J. Sediment. Res.* 70, 1197–1209. <https://doi.org/10.1306/012400701197>
- Rao, P. V., Mohan Rao, K., Vora, K.H., Almeida, F., Subramaniam, M.M., Godfrey, C., Souza, A., 1998. A potential phosphorite deposit on the continental margin off Chennai. *Curr. Sci.* 74, 574–577.
- Redfield, A.C., 1963. The influence of organisms on the composition of seawater. *sea* 2, 26--77.
- Reimer, P.J., L Baillie, M.G., Bard, E., Bayliss, A., Beck, J.W., Blackwell, P.G., Bronk Ramsey, C., 2009. INTCAL09 AND MARINE09 RADIOCARBON AGE CALIBRATION CURVES, 0-50,000 YEARS CAL BP. *Radiocarbon* 51, 26.
- Resmi, M.R., Achyuthan, H., Jaiswal, M.K., 2017. Middle to late Holocene paleochannels and migration of the Palar River, Tamil Nadu: Implications of neotectonic activity. *Quat. Int.* 443, 211–222. <https://doi.org/10.1016/J.QUAINT.2016.05.002>
- Ruttenberg, K.C., 2003. The global phosphorus cycle. *Treatise on geochemistry* 8, 682.
- Ruttenberg, K.C., 1992. Development of a Sequential Extraction Method for Different Forms of Phosphorus in Marine Sediments. *Limnol. Oceanogr.* 37, 1460–1482. <https://doi.org/10.4319/lo.1992.37.7.1460>
- Ruttenberg, K.C., Berner, R.A., 1993. Authigenic apatite formation and burial in sediments from non-upwelling, continental margin environments. *Geochim. Cosmochim. Acta* 57, 991–1007. [https://doi.org/10.1016/0016-7037\(93\)90035-U](https://doi.org/10.1016/0016-7037(93)90035-U)
- Ruttenberg, K.C., Goñi, M.A., 1997. Phosphorus distribution, C:N:P ratios, and $\delta^{13}\text{C}_{\text{oc}}$ in arctic, temperate, and tropical coastal sediments: tools for characterizing bulk sedimentary organic matter. *Mar. Geol.* 139, 123–145. [https://doi.org/10.1016/S0025-3227\(96\)00107-7](https://doi.org/10.1016/S0025-3227(96)00107-7)
- Ruttenberg, K.C., Sulak, D.J., 2011. Sorption and desorption of dissolved organic phosphorus onto iron (oxyhydr)oxides in seawater. *Geochim. Cosmochim. Acta* 75, 4095–4112. <https://doi.org/10.1016/J.GCA.2010.10.033>
- Sardesai, S., Ramaiah, N., Kumar, S.P., de Sousa, S.N., 2007. Influence of environmental forcings on the seasonality of dissolved oxygen and nutrients in the Bay of Bengal. *J. Mar. Res.* 65, 301–316.
- Sarma, V.V.S.S., 2022. Biogeochemistry of carbon, nitrogen and oxygen in the Bay of Bengal: New insights through re-analysis of data. *J. Earth Syst. Sci.* 131. <https://doi.org/10.1007/s12040-022-01915-z>

- Sarma, V.V.S.S., Krishna, M.S., Viswanadham, R., Rao, G.D., Rao, V.D., Sridevi, B., Kumar, B.S.K., Prasad, V.R., Subbaiah, C. V., Acharyya, T., Bandopadhyay, D., 2013. Intensified oxygen minimum zone on the western shelf of Bay of Bengal during summer monsoon: Influence of river discharge. *J. Oceanogr.* 69, 45–55. <https://doi.org/10.1007/s10872-012-0156-2>
- Sarma, V.V.S.S., Vivek, R., Rao, D.N., Ghosh, V.R.D., 2020. Severe phosphate limitation on nitrogen fixation in the Bay of Bengal. *Cont. Shelf Res.* 205. <https://doi.org/10.1016/J.CSR.2020.104199>
- Sastri, V. V., Venkatachala, B.S., Narayanan, V., 1981. The evolution of the east coast of India. *Palaeogeogr. Palaeoclimatol. Palaeoecol.* 36, 23–54. [https://doi.org/10.1016/0031-0182\(81\)90047-X](https://doi.org/10.1016/0031-0182(81)90047-X)
- Schenau, S.J., De Lange, G.J., 2001. Phosphorus regeneration vs. burial in sediments of the Arabian Sea. *Mar. Chem.* 75, 201–217. [https://doi.org/10.1016/S0304-4203\(01\)00037-8](https://doi.org/10.1016/S0304-4203(01)00037-8)
- Schenau, S.J., De Lange, G.J., 2000. A novel chemical method to quantify fish debris in marine sediments. *Limnol. Ocean.* 45, 963–971. <https://doi.org/10.4319/lo.2000.45.4.0963>
- Schenau, S.J., Reichert, G.J., De Lange, G.J., 2005. Phosphorus burial as a function of paleoproductivity and redox conditions in Arabian Sea sediments. *Geochim. Cosmochim. Acta* 69, 919–931. <https://doi.org/10.1016/J.GCA.2004.05.044>
- Schenau, S.J., Slomp, C.P., De Lange, G.J., 2000. Phosphogenesis and active phosphorite formation in sediments from the Arabian Sea oxygen minimum zone. *Mar. Geol.* 169, 1–20. [https://doi.org/10.1016/S0025-3227\(00\)00083-9](https://doi.org/10.1016/S0025-3227(00)00083-9)
- Sebastian, T., Nath, B.N., Miriyala, P., Linsy, P., Kocherla, M., 2023. Climatic control on detrital sedimentation in the continental margin off Chennai, western Bay of Bengal – A 42 kyr record. *Palaeogeogr. Palaeoclimatol. Palaeoecol.* 609, 111313. <https://doi.org/10.1016/j.palaeo.2022.111313>
- Sebastian, T., Nath, B.N., Ramaswamy, V., Mascarenhas-Pereira, M.B.L., Yazing, A.K., Apurva, P.R., Linsy, P., Kocherla, M., Miriyala, P., Rao, B.R., 2019. Distribution and dispersal of surface sediments on the continental margins of India. *Mar. Pet. Geol.* 110. <https://doi.org/10.1016/j.marpetgeo.2019.07.017>
- Simpson, H., Broecker, W., Garrels, R., Gessel, S., Holland, H., Holser, W., Junge, C., Kaplan, I., McElroy, M., Michaelis, W., Others, 1977. Man and the global nitrogen cycle group report, in: *Global Chemical Cycles and Their Alterations by Man. Report of the Dahlem Workshop on Global Chemical Cycles and Their Alterations by Man (Berlin 15--19 November 1976)*. Physical and Chemical Sciences Research Reports. pp. 253–274.
- Slomp, C.P., Van Der Gaast, S.J., Van Raaphorst, W., 1996. Phosphorus binding by poorly crystalline iron oxides in North Sea sediments. *Mar. Chem.* 52, 55–73. [https://doi.org/10.1016/0304-4203\(95\)00078-X](https://doi.org/10.1016/0304-4203(95)00078-X)
- Southon, J., Kashgarian, M., Fontugne, M., Metivier, B., Yim, W.W.S., 2002. Marine Reservoir Corrections for the Indian Ocean and Southeast Asia. *Radiocarbon* 44, 167–180. <https://doi.org/10.1017/S0033822200064778>

- Stoll, H.M., Arevalos, A., Burke, A., Ziveri, P., Mortyn, G., Shimizu, N., Unger, D., 2007. Seasonal cycles in biogenic production and export in Northern Bay of Bengal sediment traps. *Deep. Res. II* 54, 558–580. <https://doi.org/10.1016/j.dsr2.2007.01.002>
- Strickland, J.D., Parsons, T.R., 1972. A practical handbook of seawater analysis, 2nd ed. Fisheries Research Board of Canada.
- Subramanian, V., Van 't Dack, L., Van Grieken, R., 1985. Chemical composition of river sediments from the Indian sub-continent. *Chem. Geol.* 48, 271–279. [https://doi.org/10.1016/0009-2541\(85\)90052-X](https://doi.org/10.1016/0009-2541(85)90052-X)
- Suess, E., 1981. Phosphate regeneration from sediments of the Peru continental margin by dissolution of fish debris. *Geochim. Cosmochim. Acta* 45, 577–588. [https://doi.org/10.1016/0016-7037\(81\)90191-5](https://doi.org/10.1016/0016-7037(81)90191-5)
- Susanth, S., John Kurian, P., Twinkle, D., Bijesh, C.M., Tyagi, A., 2021a. Potential submarine landslide zones off Chennai, Southeast Continental Margin of India. *Reg. Stud. Mar. Sci.* 45, 101832. <https://doi.org/10.1016/j.rsma.2021.101832>
- Susanth, S., Kurian, P.J., Bijesh, C.M., Twinkle, D., Tyagi, A., Rajan, S., 2021b. Controls on the evolution of submarine canyons in steep continental slopes: geomorphological insights from Palar Basin, southeastern margin of India. *Geo-Marine Lett.* 41. <https://doi.org/10.1007/s00367-021-00685-9>
- Symphonia, K.T., Nathan, D.S., 2018. Geochemistry and distribution of sediments in the East Indian shelf, SW Bay of Bengal: implications on weathering, transport and depositional environment. *J. Earth Syst. Sci.* 127, 1–18. <https://doi.org/10.1007/s12040-018-0999-z>
- Tripathy, G., Singh, S., Ramaswamy, V., 2014. Major and trace element geochemistry of Bay of Bengal sediments: Implications to provenances and their controlling factors. *Palaeogeogr. Palaeoclimatol. Palaeoecol.* 397, 20–30. <https://doi.org/10.1016/j.palaeo.2013.04.012>
- Twinkle, D., Srinivasa Rao, G., Radhakrishna, M., Murthy, K.S.R., 2016. Crustal structure and rift tectonics across the cauvery–palar basin, eastern continental margin of india based on seismic and potential field modelling. *J. Earth Syst. Sci.* 125, 329–342. <https://doi.org/10.1007/S12040-016-0669-Y/FIGURES/7>
- Tyrrell, T., 1999. The relative influences of nitrogen and phosphorus on oceanic primary production. *Nature* 400, 525–531.
- Van Cappellen, P., Berner, R.A., 1988. A mathematical model for the early diagenesis of phosphorus and fluorine in marine sediments; apatite precipitation. *Am. J. Sci.* 288, 289–333.
- van der Zee, C., Slomp, C.P., van Raaphorst, W., 2002. Authigenic P formation and reactive P burial in sediments of the Nazaré canyon on the Iberian margin (NE Atlantic). *Mar. Geol.* 185, 379–392. [https://doi.org/10.1016/S0025-3227\(02\)00189-5](https://doi.org/10.1016/S0025-3227(02)00189-5)
- Vaz, G., Vijaykumar, P., Rao, B.L., 1999. Phosphorite from the continental margin off madras, bay of bengal. *Mar. Georesources Geotechnol.* 17, 33–48. <https://doi.org/10.1080/106411999273990>

- Vaz, G.G., 1995. Phosphatic nodules in the outer continental shelf off Madras, Bay of Bengal. *Indian J. Mar. Sci.* 24, 8–12.
- Viktorsson, L., Ekeröth, N., Nilsson, M., Kononets, M., Hall, P.O.J.J., 2013. Phosphorus recycling in sediments of the central Baltic Sea. *Biogeosciences* 10, 3901–3916. <https://doi.org/10.5194/bg-10-3901-2013>
- Wang, D., Zhu, M.X., Yang, G.P., Ma, W.W., 2019. Reactive Iron and Iron-Bound Organic Carbon in Surface Sediments of the River-Dominated Bohai Sea (China) Versus the Southern Yellow Sea. *J. Geophys. Res. Biogeosciences* 124, 79–98. <https://doi.org/10.1029/2018JG004722>
- Watanabe, F.S.T., Olsen, S., 1962. Colorimetric determination of phosphorus in water extracts of soil. *Soil Sci.* 93, 183–188.
- Yang, B., Song, G.-D., Liu, S.M., Jin, J., 2017. Phosphorus recycling and burial in core sediments of the East China Sea. *Mar. Chem.* 192, 59–72.
- Zhu, M.-X., Hao, X.-C., Shi, X.-N., Yang, G.-P., Li, T., 2012. Speciation and spatial distribution of solid-phase iron in surface sediments of the East China Sea continental shelf. *Appl. Geochemistry* 27, 892–905. <https://doi.org/10.1016/j.apgeochem.2012.01.004>

Table 1: Radiocarbon ages for the dated sections of sediment cores along with lab reference codes (Inter-University Accelerator Centre (IUAC), Delhi). The measured radiocarbon ages were corrected for a regional reservoir correction of 0.356 kyr for the western Bay of Bengal (Southon et al., 2002) and calibrated into calendar ages using CALIB 8.1.0 online software program (Reimer et al., 2009) along with the MARINE20 dataset.

Sample Name	Lab Reference Number	Radiocarbon Age (Kyr BP)	Calibrated Age (Kyr BP)
SPC5/ 2.5 cm	IUACD#22C5000	7.355±0.031	7.313 ± 0.175
SPC5/ 25.5 cm	IUACD#22C5001	10.439±0.036	10.994 ± 0.230
SPC7/ 18.5 cm	IUACD#22C5002	8.551±0.033	8.504 ± 0.210
SPC13/ 2.5 cm	IUACD#22C5003	2.966±0.024	2.124 ± 0.200
SPC13/ 27cm	IUACD#22C5004	3.417±0.026	2.682 ± 0.210
SPC3/ 15.5cm	IUACD#22C5005	3.213±0.025	2.440 ± 0.220

Table 2: Table showing bottom water dissolved oxygen concentration, bottom water DIP, porewater DIP at the sediment-water interface and diffusive flux of phosphate and C_{org} and $CaCO_3$ in the core top sediments (0-1cm),

Station Name	Latitude °N	Longitude °E	Water depth (m)	Bottom water dissolved oxygen ($\mu\text{mol/L}$)	C_{org} (wt.%)	$CaCO_3$ (wt.%)	Bottom water DIP ($\mu\text{mol/L}$)	Porewater DIP at the sediment-water interface ($\mu\text{mol/L}$)	Benthic Flux of Phosphate ($\mu\text{mol cm}^{-2} \text{yr}^{-1}$)	Burial Efficiency (PBE) (%)
SSK50/SPC5	12.10	92.88	269	11.7	1.87	13.6	2.73	7.75	0.53	12.6
SSK50/SPC7	12.99	80.63	202	9.9	2.00	22.7	2.19	18.72	1.50	23.3
SSK50/SPC13	11.39	79.94	218	12.0	1.16	5.9	2.51	32.36	-	-
SSK59/SPC3	11.37	80.00	224	8.3	0.31	6.4	0.65	25.00	1.13	48.2

Figure Captions

Figure 1: An overview map of the southeastern margin of India showing Palar Basin and Cauvery Basin, respectively (topography from Becker et al., 2009). The paleochannels of Palar river in the inland region identified through remote sensing studies (Resmi et al., 2017) are overlain. The offshore region illustrates the location of the spade core samples (red diamond), Phosphorite bearing zone in the outer shelf off Chennai (Vaz, 1995) and the Palar Canyon System in the continental slope (modified after Susanth et al., 2021)

Figure 2: Downcore variation of C_{org} , $CaCO_3$ and N_{total} (units wt.%) measured in bulk sediment.

Figure 3: Downcore variation of molar C_{org}/N_{total} , C_{org}/P_{org} , C_{org}/P_{react} ratios in sediments and dissolved phosphate ($\mu\text{mol/L}$) in porewater.

Figure 4: Down core variation of total phosphorus and P in five geochemically separable phases (units in $\mu\text{mol/g}$) of sediments.

Figure 5: Relative percentages of solid P phases separated by sequential chemical extraction with sediment depth

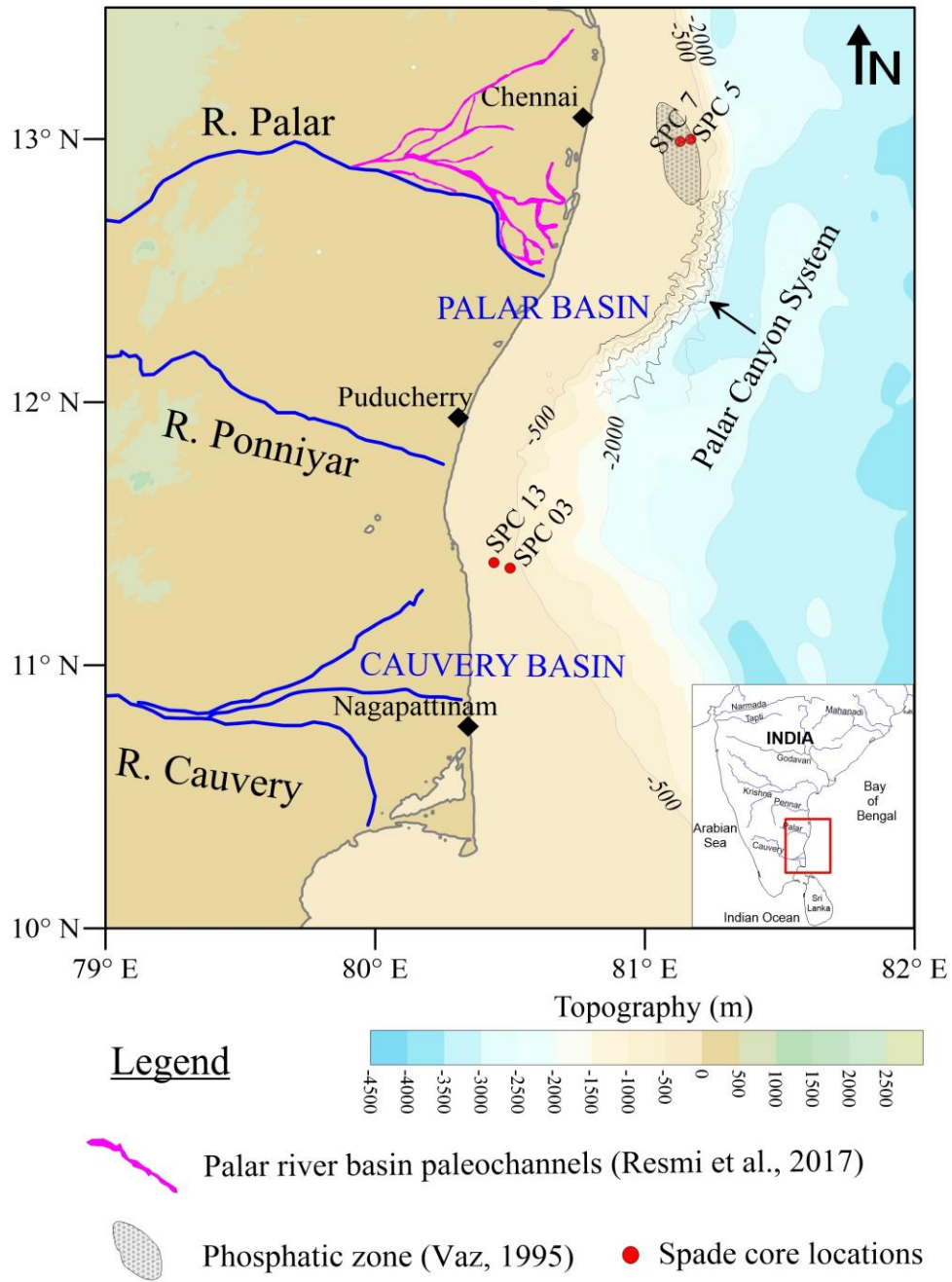
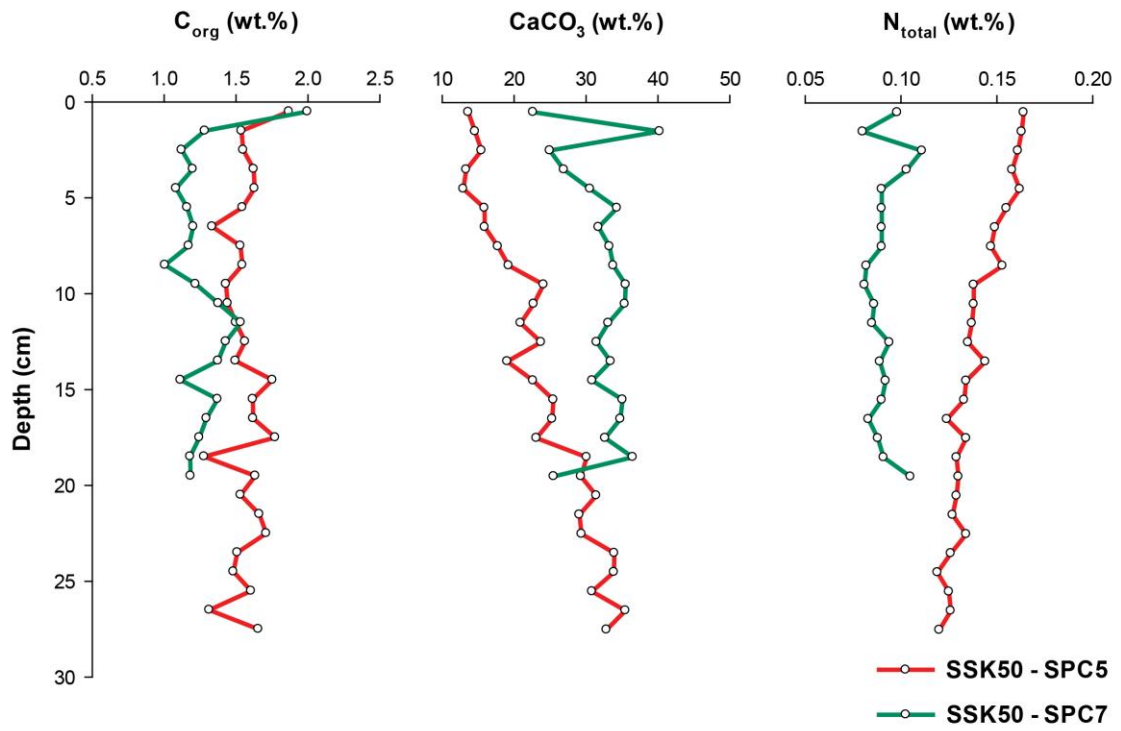


Figure 1

(a) Phosphatic Zone - Palar Basin



(b) Non-phosphatic Zone - Cauvery Basin

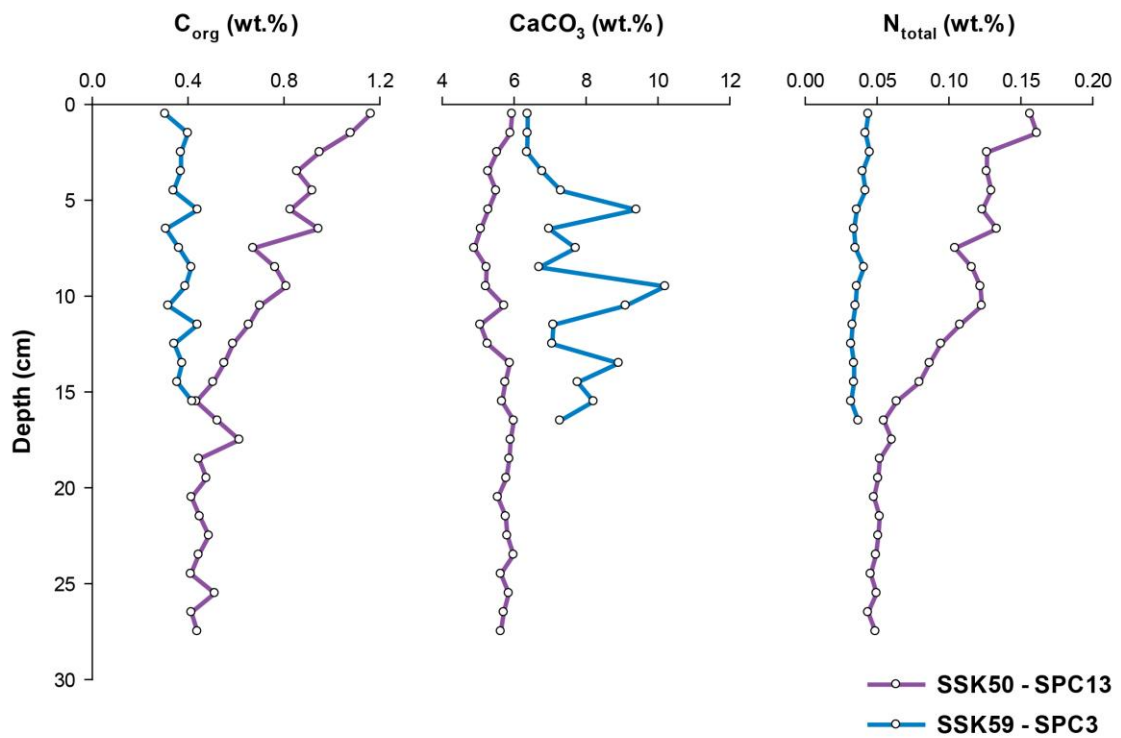
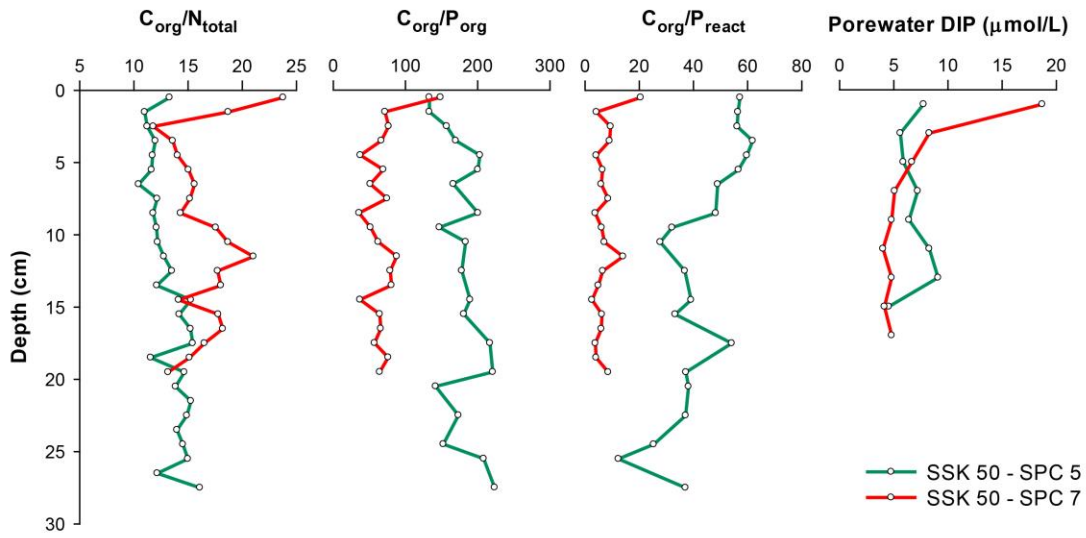


Figure 2

(a) Palar Basin



(b) Cauvery Basin

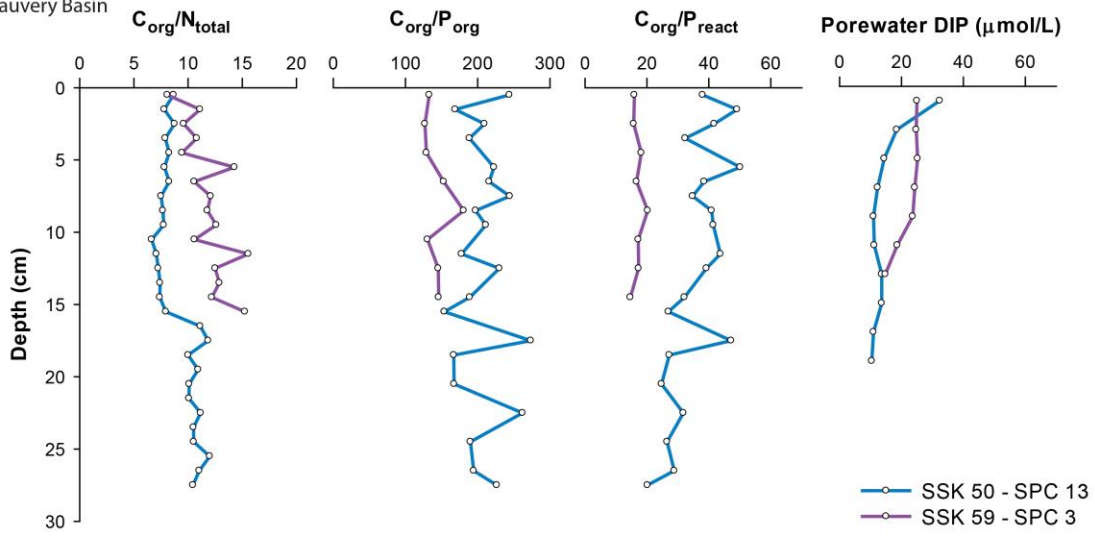


Figure 3

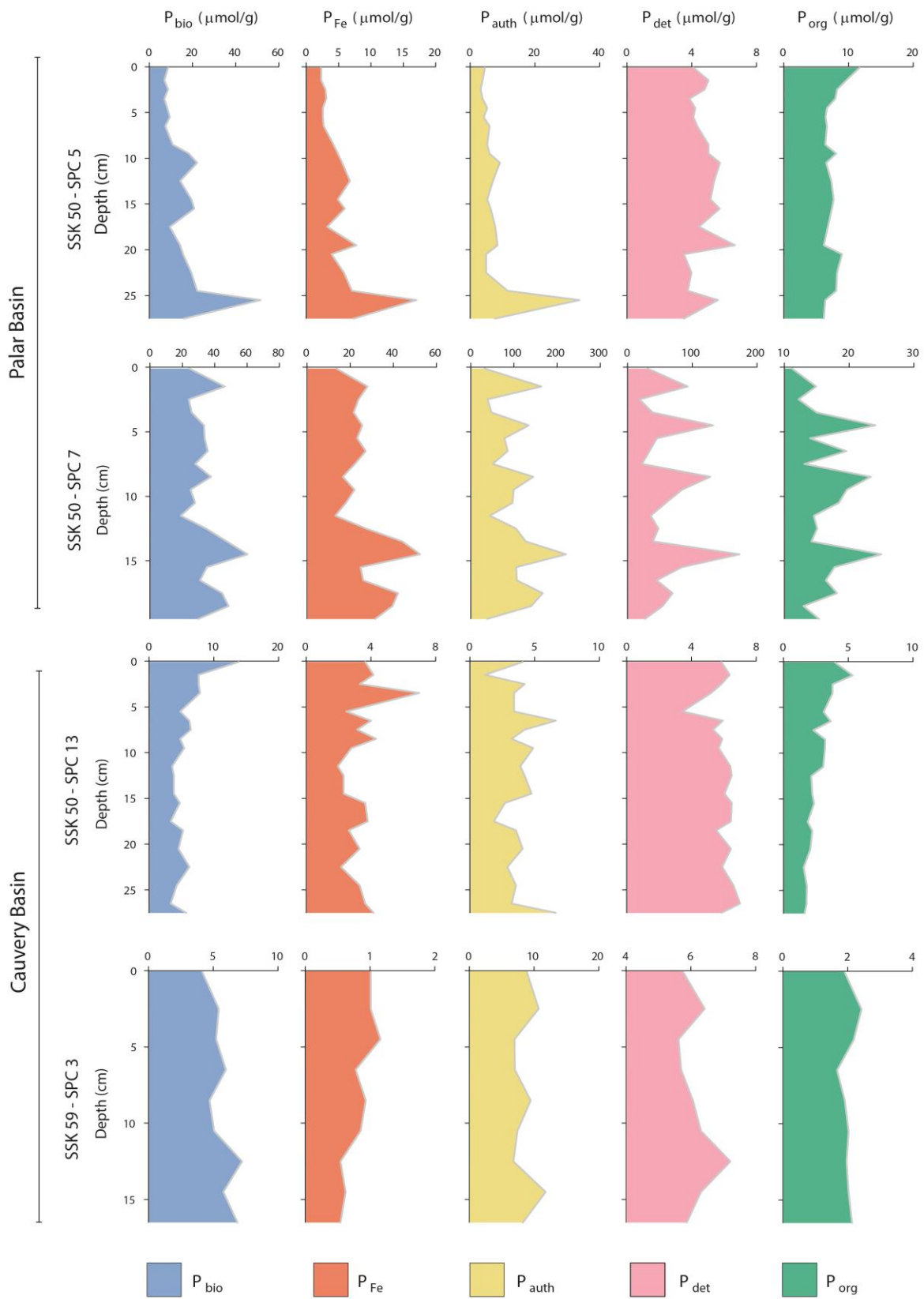


Figure 4

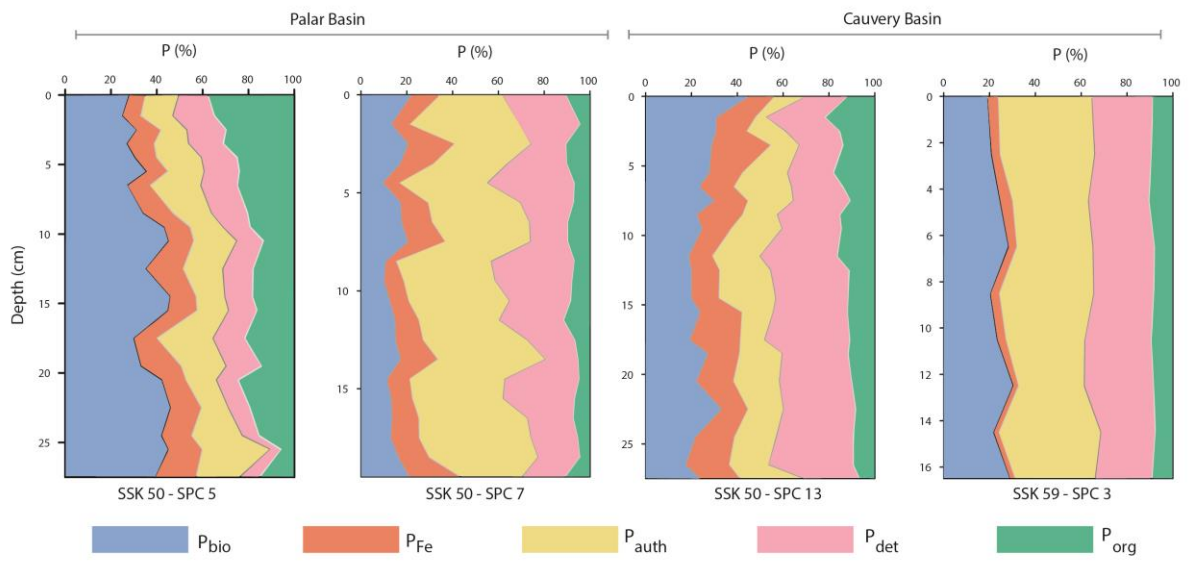


Figure 5